Thermodynamic Properties of 1-Butyl-3-methylimidazolium Hexafluorophosphate in the Condensed State

Gennady J. Kabo,* Andrey V. Blokhin, Yauheni U. Paulechka, Andrey G. Kabo, and Marina P. Shymanovich

Belarusian State University, Chemical Faculty, Leningradskaya 14, Minsk 220050, Belarus

Joseph W. Magee

Physical and Chemical Properties Division, National Institute of Standards and Technology, 325 Broadway, Boulder, Colorado 80305-3328

Thermodynamic functions for 1-butyl-3-methylimidazolium hexafluorophosphate ([C_4mim][PF_6]) are reported in a range of temperatures from (5 to 550) K, based on new measurements by calorimetry. Heat capacities of the crystal, glass, and liquid phases for [C_4mim][PF_6] were measured with a pair of calorimeters. A vacuum-jacketed adiabatic calorimeter was used at temperatures between (5 and 310) K, and a heat bridge-scanning calorimeter was used from (300 to 550) K. With the adiabatic calorimeter, the fusion T_{fus} = 283.51 K, $\Delta^1_{cr} H^\circ_m$ = 19.60 kJ·mol^{-1}, and the glass transition T_g = 190.6 K were observed. The [C_4mim][PF_6] test sample was determined to have a mole fraction purity of 0.9956 by a fractional melting analysis. Densities of the liquid were measured in a range of temperatures from (298 to 353) K with a pycnometer equipped with a capillary neck. An unexpected endothermal transition, with a very small enthalpy change of 0.25 J·g^{-1} (0.071 kJ·mol^{-1}), was observed in a range of temperatures from (394 to 412) K. Heat capacity jumps were determined at the glass transition $\Delta^1_{gl} C_s$ = 81.6 J·K^{-1}·mol^{-1} and fusion $\Delta^1_{cr} C_s$ = 44.8 J·K^{-1}·mol^{-1}, and the observed entropy change at fusion is $\Delta^1_{cr} S$ (283.51 K) = 69.23 J·K^{-1}·mol^{-1}.

Introduction

Room-temperature ionic liquids (RTIL) have attracted considerable attention due to their potential uses by the chemical industry as environmentally friendly and selective solvents for chemical reactions and homogeneous catalysis[1], extraction[2], separation of substances,[3] and electrochemical processes.[4] RTIL can decrease expenses caused by loss of volatile organic solvents and pollution of the environment.[4]

Investigation of thermodynamic properties of RTIL should favor examination of their structure and substantiation of technologies for their synthesis and use. However, not one RTIL has been investigated to determine its thermodynamic properties in full measure. In a companion work,[5] we reported theoretical calculations of thermodynamic properties of 1-butyl-3-methylimidazolium hexafluorophosphate ([C_4mim][PF_6]) in the ideal gas state in a range of temperatures from (50 to 1500) K. We also discussed the thermal stability of [C_4mim][PF_6] from the standpoint of the slow heating rates used in calorimetric measurements.

To interpret any physical property measurement on an RTIL sample, a knowledge of its purity is essential. In this work, fractional melting is used to determine the purity of the [C_4mim][PF_6] test sample. Also, we report measurements of heat capacity in the condensed state for [C_4mim][PF_6] in the temperature range from (5 to 300) K by adiabatic calorimetry and from (300 to 500) K by scanning calorimetry. Thermodynamic properties for both the fusion and glass transition are also reported.

* To whom correspondence may be addressed.

The temperature dependence of the heat capacity of [C_4mim][PF_6] is shown to differ from the usual dependence observed for both molecular liquids and ionic crystals. The largest difference is an anomalously large specific heat capacity below 50 K. Such an anomaly could be explained either by unusually low values of characteristic temperatures for the [C_4mim][PF_6] crystal or by an unusually large electronic contribution to the heat capacity in this temperature range.

Experimental Section

Chemicals. A commercial sample of [C_4mim][PF_6] from Covalent Associates, Inc., was treated before measurements, as previously described in a companion study.[5] (We provide trade names only as needed for complete scientific description; their use does not imply an endorsement by the National Institute of Standards and Technology. Other products could perform equally well.) The final purity of the treated sample that was used in the tests was determined to be 0.9956 mol fraction, as described in the Results section. The original sample was certified by the supplier to be of electrochemical grade with impurities of <50 ppm Cl^- ion and <50 ppm H_2O. In-house tests were made to see if these impurity levels could be confirmed. A semiquantitative $AgNO_3$ test found that the Cl^- concentration was below the detection limit of 100 ppm. This finding was confirmed by a test with a Cl^--selective electrode, which showed that the Cl^- concentration was below the detection limit of 130 ppm. For Cl^--selective electrode tests on [C_4mim][PF_6], the instrument's stated detection limit of 2 ppm could not be realized due to the limited solubility of [C_4mim][PF_6] in the aqueous solution that was tested. An ^{19}F

10.1021/je034102r CCC: $27.50
Published on Web 04/09/2004

NMR test showed that the sample purity was 0.999 mol fraction and that hydrolysis of the PF_6^- anion had not been a problem during sample storage. An ^1H NMR test of the original [C_4mim][PF_6] dissolved in a deuterated solvent CD_3CN showed the presence of three minor impurities (plus H_2O) that originated from the ionic liquid. A solvent blank test revealed three other minor impurities (plus H_2O) that originated from the NMR solvent. The calculated purity (excluding H_2O) of the original [C_4mim][PF_6] sample is 0.9995 mol fraction. Despite the great care taken to avoid introducing contaminants to the original sample, it appears that some H_2O was inadvertently introduced by handling the sample. Two Karl Fischer titrations revealed H_2O concentrations of 411 and 412 ppm by mass (0.0004 mass fraction or ~0.006 mol fraction) in the stored [C_4mim][PF_6]. The H_2O would need to be removed prior to measurements. As reported in the companion study, we vacuum pumped the sample, first at 293 K for 3 h and then at 430 K for 10 h, to remove volatile impurities. The total observed mass loss was 0.0016 mass fraction, an amount that is four times the H_2O concentration determined by Karl Fischer titration. This finding suggests that, in addition to H_2O, unidentified volatile impurities were present prior to treatment of the sample. One could easily speculate that dissolved components of air (N_2, O_2, Ar, CO_2) contributed to the observed volatile impurities. The absence of free H_2O in our treated sample was confirmed by a subsequent study of the sample with the Knudsen effusion technique, which concluded that the vapor pressure at $T < 430$ K was less than the observation threshold of 10^{-2} Pa. The treated sample was used in the experiments.

Apparatus and Procedures. Heat capacities in the temperature range (5 to 310) K in the condensed state and enthalpy of fusion of [C_4mim][PF_6] were measured with a vacuum adiabatic calorimeter TAU−1 built by VNIIFTRI (Moscow) as already described.[6−8] A liquid sample with a mass of 1.28614 g was loaded into a stainless steel container of 1.0 cm^3 volume with a helium-filled headspace. The container was sealed with an indium ring. The temperature was measured with an iron−rhodium resistance thermometer ($R_0 = 101.83$ Ω) located on the inner surface of the adiabatic shield and calibrated for ITS-90 by VNIIFTRI. Adiabatic conditions were maintained with a four-junction differential thermocouple as an indicator of the temperature difference between the shield and the calorimetric cell.

The accuracy of the heat capacity measurements was indicated previously in experiments with benzoic acid[9,10] (K−1 grade, mass fraction ≥ 0.99995) and with high-purity copper[11] (mass fraction ≥ 0.99995). The estimated expanded uncertainty with a coverage factor ($k = 2$) of the measured molar heat capacity $C_{s,m}$ is ±0.4% over the temperature range (40 to 320) K. The uncertainty becomes larger at $T < 40$ K, finally reaching ±2% near 5 K. The reliability of the calorimeter was also confirmed by the good agreement of the results of our heat capacity measurements for cyclopentanol[12] between temperatures of (80 and 300) K and chlorocyclohexane[13] between temperatures of (10 and 300) K with the results of other authors.[14,15] In the present study, the difference between the values of $C_{s,m}$ and $C_{p,m}$ is considered to be negligible due to the extremely low (≪1 Pa) vapor pressure of [C_4mim][PF_6].

The heat capacity of [C_4mim][PF_6] in the range (300 to 550) K was measured in an improved automatic scanning calorimeter of the heat bridge type.[16] The calorimeter was calibrated with high-purity copper (mass fraction ≥ 0.99995). The expanded uncertainty of the heat capacity measurements is estimated to be ±2%. The mass of the sample was 1.0834 g. The container with the sample was hermetically sealed in a vacuum. The average heating rate was 0.8 K·min^{-1}.

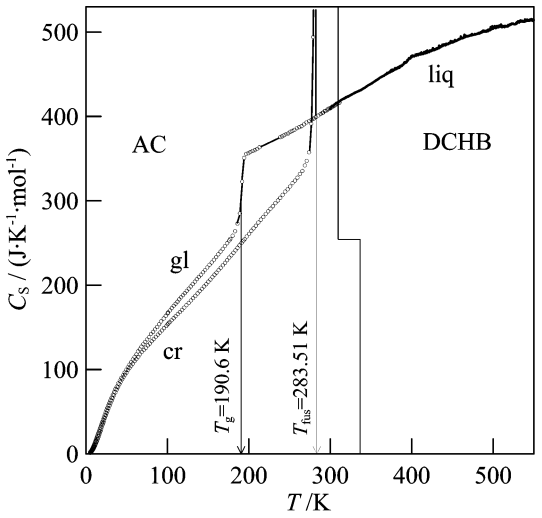

Figure 1. Heat capacity of [C_4mim][PF_6] in the crystalline, glassy, and liquid states. AC is range of the adiabatic calorimeter, DCHB is the range of the heat bridge-scanning calorimeter, T_g is the glass transition temperature, and T_{fus} is the triple-point temperature.

The density of liquid [C_4mim][PF_6] was measured pycnometrically. The pycnometer had a capillary neck (1 mm diameter) with flat top. The temperature dependence of the volume of the pycnometer is given by

$$V_1/\mathrm{cm}^3 = (1.21542 \pm 0.00007) + (1.8 \pm 0.1) \times 10^{-5}(T/\mathrm{K} - 273.15) \quad (1)$$

which was determined from a calibration with degassed, twice-distilled water; the correlation coefficient of the fit to eq 1 is $r^2 = 0.976$. The pycnometer was placed inside a copper block that was immersed in a liquid thermostatic bath. The temperature was controlled within ±0.02 K. The temperature of the block was measured with a calibrated mercury thermometer.

The pycnometer was first completely filled with degassed liquid [C_4mim][PF_6] at about 293 K, covered with a cap, and then thermostated for at least 10 min. After each temperature step, the excess liquid resulting from thermal expansion was removed from the top of the neck of the pycnometer with a Teflon palette knife. After the excess liquid was removed, the pycnometer's neck was covered with a Teflon cap in order to prevent gas absorption. Then the pycnometer was cooled to 293 K and weighed on an electronic balance with an uncertainty ±5 × 10^{-5} g. Measurements were performed at temperatures from (298 to 353) K. The expanded uncertainty of density measurements is estimated to be ±2 × 10^{-4} g·cm^{-3} (approximately 0.02%), before accounting for possible effects of impurities since these could not be quantified.

Results

Experimental values of the molar heat capacities of [C_4mim][PF_6] in the range (5 to 550) K are shown in Figure 1. The experimental heat capacities obtained by adiabatic calorimetry are presented in Table 1. The temperature intervals for measurements of the values of $C_{s,m}$ are close to the differences between the mean temperatures of two consecutive experiments in the series of measurements.

Table 1. Experimental Molar Heat Capacities $C_{s,m}$ at Vapor-Saturation Pressure for 1-Butyl-3-methylimidazolium Hexafluorophosphate (R = 8.314 472 J·K^{-1}·mol^{-1})

$\langle T\rangle$/K	$C_{s,m}/R$	$\langle T\rangle$/K	$C_{s,m}/R$	$\langle T\rangle$/K	$C_{s,m}/R$	$\langle T\rangle$/K	$C_{s,m}/R$	$\langle T\rangle$/K	$C_{s,m}/R$	$\langle T\rangle$/K	$C_{s,m}/R$	$\langle T\rangle$/K	$C_{s,m}/R$	$\langle T\rangle$/K	$C_{s,m}/R$
Series 1 Liquid															
290.53	48.62	293.21	48.86	296.25	48.99	299.28	49.27	302.31	49.50	305.32	49.66	308.31	49.87	311.31	50.07
Series 2 Supercooled Liquid															
279.27	47.78	282.28	48.02												
Series 2 Liquid															
285.27	48.24	291.29	48.65	294.38	48.92	297.45	49.19	300.51	49.29	303.56	49.53	306.66	49.79	309.81	50.03
288.25	48.46														
Series 3 Glass															
100.78	20.15	112.28	21.68	123.71	23.24	136.20	24.91	148.93	26.57	162.53	28.46	176.04	30.43	188.97	34.28
103.17	20.45	114.54	22.03	126.20	23.55	138.67	25.23	151.70	26.96	165.29	28.84	177.26	30.64	191.70	38.82
105.51	20.79	116.84	22.33	128.66	23.86	141.19	25.54	154.44	27.29	168.02	29.24	180.15	31.11	194.24	42.21
107.81	21.10	119.11	22.63	131.16	24.21	143.75	25.89	157.14	27.67	170.72	29.63	183.09	31.74		
110.06	21.40	121.35	22.91	133.70	24.55	146.28	26.21	159.81	28.05	173.39	30.03	186.06	32.83		
Series 3 Supercooled Liquids															
196.80	42.76	199.36	42.87	201.91	43.04	204.58	43.19	207.37	43.31	210.22	43.47	213.13	43.71		
Series 4 Crystal															
100.28	18.47	120.60	20.85	142.43	23.53	162.92	26.20	183.56	29.01	203.07	31.80	226.59	34.96	250.71	38.12
102.77	18.77	123.41	21.20	145.07	23.87	165.46	26.53	186.06	29.38	205.82	32.16	229.55	35.31	253.70	38.60
105.21	19.06	126.17	21.52	147.68	24.19	168.07	26.89	188.53	29.73	208.72	32.53	232.58	35.74	256.67	38.96
107.60	19.34	128.89	21.87	150.26	24.55	170.71	27.23	190.98	30.05	211.76	32.99	235.59	36.13	259.68	39.38
110.13	19.62	131.56	22.20	152.80	24.86	173.34	27.61	193.42	30.41	214.78	33.40	238.56	36.51	262.73	39.91
112.77	19.94	134.28	22.52	155.32	25.21	175.93	27.99	194.81	30.61	217.77	33.79	241.58	36.93	265.76	40.33
115.37	20.22	137.03	22.87	157.81	25.54	178.50	28.31	197.49	31.00	220.73	34.20	244.65	37.38	268.75	41.13
117.92	20.53	139.75	23.21	160.34	25.84	181.04	28.66	200.29	31.37	223.67	34.57	247.69	37.71		
Series 5 Supercooled Liquids															
238.61	45.16	243.49	45.43	248.49	45.69	253.43	46.04	258.86	46.43	264.77	46.72	270.75	47.25	277.07	47.65
240.98	45.27	246.00	45.60	250.97	45.93	256.03	46.20	261.82	46.59	267.70	46.98	273.92	47.44	280.22	47.84
Series 6 Glass															
5.09	0.2464	8.21	0.8368	12.81	2.169	20.17	4.586	31.43	8.001	49.44	11.99	70.41	15.64	95.42	19.30
5.36	0.2809	8.61	0.9348	13.36	2.351	21.05	4.886	32.95	8.427	51.38	12.35	72.69	15.97	97.92	19.67
5.59	0.3159	9.00	1.038	13.99	2.550	22.07	5.233	34.52	8.834	53.34	12.71	75.03	16.31	100.38	20.03
5.85	0.3604	9.41	1.153	14.65	2.768	23.08	5.539	36.17	9.232	55.43	13.08	77.42	16.65		
6.14	0.4102	9.82	1.258	15.35	3.000	24.15	5.902	37.88	9.596	57.60	13.46	79.89	17.09		
6.47	0.4617	10.27	1.400	16.07	3.229	25.25	6.232	39.66	10.04	59.75	13.82	82.45	17.38		
6.82	0.5357	10.76	1.532	16.81	3.473	26.28	6.567	41.55	10.45	61.89	14.17	84.93	17.76		
7.15	0.5945	11.23	1.685	17.63	3.745	27.38	6.886	43.54	10.86	64.01	14.62	87.39	18.08		
7.49	0.6731	11.74	1.828	18.50	4.033	28.63	7.228	45.53	11.22	66.11	14.90	89.83	18.49		
7.84	0.7547	12.29	2.002	19.36	4.321	29.99	7.622	47.48	11.61	68.19	15.30	92.25	18.89		
Series 7 Crystal															
5.13	0.1281	8.28	0.5286	12.92	1.694	20.45	4.177	31.51	7.595	48.00	11.29	68.68	14.52	93.26	17.59
5.41	0.1480	8.66	0.6001	13.56	1.891	21.38	4.478	32.97	7.982	49.81	11.59	71.13	14.80	95.87	17.93
5.67	0.1690	9.07	0.6903	14.20	2.076	22.32	4.787	34.47	8.359	51.62	11.95	73.64	15.13	98.65	18.24
5.97	0.1955	9.49	0.7792	14.85	2.292	23.31	5.120	36.07	8.749	53.48	12.25	76.05	15.47	101.35	18.63
6.29	0.2318	9.92	0.8842	15.51	2.497	24.37	5.479	37.71	9.155	55.49	12.56	78.39	15.73		
6.60	0.2723	10.35	0.9856	16.24	2.739	25.51	5.833	39.38	9.539	57.62	12.86	80.75	16.06		
6.91	0.3086	10.75	1.083	17.00	2.987	26.64	6.161	41.07	9.918	59.71	13.22	83.19	16.36		
7.23	0.3601	11.18	1.208	17.78	3.244	27.83	6.525	42.76	10.28	61.89	13.51	85.74	16.68		
7.58	0.4131	11.74	1.358	18.66	3.548	29.06	6.899	44.47	10.63	64.13	13.84	88.31	17.01		
7.92	0.4628	12.32	1.512	19.54	3.861	30.21	7.235	46.22	10.99	66.36	14.21	90.82	17.29		

It was found that when liquid [C_4mim][PF_6] was cooled from (290 to 300) K at a rate of (0.02 to 0.03) K·s^{-1} it was supercooled to temperatures well below the temperature of fusion, eventually forming a glassy state that was stable at a temperature of 100 K. A spontaneous crystallization of the supercooled liquid was observed when the glassy sample was heated to temperatures greater than 213 K. Thus, to obtain a completely crystalline sample in the calorimeter, a liquid sample was cooled from (290 to 300) K to 100 K, then it was heated to (260−262) K and was held at this temperature for (3−4) h until the spontaneous evolution of heat due to crystallization had ceased to be observed. Heat capacity of [C_4mim][PF_6] in the supercooled liquid state up to 213 K was measured immediately after the transition from the glass into the supercooled liquid (Table 1, series 3). The heat capacity of the supercooled liquid in a range of temperatures from (238 to 283) K was measured in two series of experiments (Table 1, series 2 and 5) after preliminary cooling of the liquid down to 278 K (series 2) and 237 K (series 5). Measurements of the heat capacities for the supercooled liquid at temperatures from (213 to 238) K were impossible since the heating of the sample during the calorimetric experiment induced crystallization of the metastable phase. Thus, heat capacities of the supercooled liquid between (213 and 238) K were obtained by an interpolation procedure; they are shown in Figure 1 with a solid line.

Table 2. Determination of the Molar Enthalpy of Melting for 1-Butyl-3-methylimidazolium Hexafluorophosphate

T_{start}/K	T_{end}/K	Q/J·mol^{-1} [a]	$\langle\Delta_{fus}H^\circ_m\rangle$/J·mol^{-1}
264.01	288.56	28352	19618
264.02	284.98	26894	19602
264.13	289.55	28668	19575
264.01	287.66	27972	19601
263.48	287.25	27993	19610
		$\langle\Delta_{fus}H^\circ_m\rangle$ =	(19601 ± 20)[b]

[a] Q is the energy needed for heating of the compound from T_{start} to T_{end}. The enthalpy of melting was calculated from the expression $\langle\Delta_{fus}H_m\rangle = Q - \int_{T_{start}}^{T_{fus}} C_{p,m}(cr)\,dT - \int_{T_{fus}}^{T_{end}} C_{p,m}(liq)\,dT$, where $C_{p,m}(cr)$ and $C_{p,m}(liq)$ are the molar heat capacities of crystal and liquid calculated by the equations $C_{p,m}(cr)/(J\cdot K^{-1}\cdot mol^{-1}) = 30.313 + 1.1456(T/K)$ and $C_{p,m}(liq)/(J\cdot K^{-1}\cdot mol^{-1}) = 304.0 + 8.855 \times 10^{-2}(T/K) + 8.807 \times 10^{-4}(T/K)^2$, which were obtained from the experimental heat capacities in the ranges (232 to 266) K for crystal and (197 to 310) K for liquid. [b] Average value.

Table 3. Results of Fractional-Melting Experiments (*f* Is the Melting Fraction at Temperature *T*)

series 1		series 2	
T/K	f	T/K	f
282.89	0.2486	282.57	0.1598
283.09	0.3687	283.14	0.3986
283.21	0.5025	283.29	0.6519
283.27	0.6378	283.32	0.7770
283.34	0.9158		

The temperature of fusion $T_{fus} = (283.51 \pm 0.01)$ K and the mole-fraction purity $x = (0.9956 \pm 0.0001)$ of [C_4mim][PF_6] were obtained from fractional melting experiments, presented in Table 3. The melted fractions f were determined after subtraction of the regular part of the heat capacity. The experimental points were fitted in terms of the van't Hoff equation

$$T = T_{fus} - \left\{\frac{RT_0^2}{\Delta_{fus}H^\circ_m}(1-x)\right\}\frac{1}{f} = (283.51 \pm 0.01) - (0.1514 \pm 0.0045)\frac{1}{f} \quad (2)$$

where T_{fus} is the temperature of fusion. The enthalpy of fusion of [C_4mim][PF_6]

$$\Delta_{fus}H^\circ_m\,(283.51\ K) = (19.60 \pm 0.02)\ kJ\cdot mol^{-1}$$

was determined in the series of independent single-step experiments, presented in Table 2. Its estimated uncertainty accounts for just those sources that arise from the calorimetric measurements, not those from any sample impurities. In each experiment, the sample was heated from a temperature difference of (19−20) K below the melting point to a temperature difference of (1−6) K above the melting point.

The experimental $C_s(T)$ curve, Figure 1, obtained by differential scanning calorimetry shows a small anomaly in the range (394−412) K with a maximum in the peak at $T = 400$ K, as shown in the heat flux curve (Figure 1, ref 5) of the companion manuscript. An enthalpy increment of 0.25 J·g^{-1} (0.071 kJ·mol^{-1}) for this peak was calculated by integration of the excess heat capacity of the compound in this temperature range. The observed endothermic anomaly can probably be attributed to hydrolysis of the [PF_6] ion by the residual H_2O in the sample. Apparently, only a small quantity of H_2O actually reacted, since the inside walls of the calorimeter were not damaged by evolving HF. More than 1500 experimental heat capacity values (with a temperature step of [0.1−0.2] K) for [C_4mim][PF_6] in the ranges (300 to 394) K and (412 to 550 K) were fitted by the polynomial

$$C_p/(J\cdot K^{-1}\cdot g^{-1}) = 0.4028 + 4.525 \times 10^{-3}(T/K) - 3.561 \times 10^{-6}(T/K)^2 \quad (3)$$

The maximum deviation of the experimental points from the smoothed curve was less than 0.6%, and the mean deviation was 0.22%.

To extrapolate the heat capacities of crystalline and glassy [C_4mim][PF_6] to $T < 5$ K, the Debye approximation

$$C_{v,m} = 3RD(\langle\Theta_D\rangle/T)$$

was used, where $\langle Q_D\rangle$ was the Debye characteristic temperature (62.7 K for the crystal and 49.5 K for the glass), which was obtained from least-squares fits of the experimental heat capacities in the regions (5.13−6.29) K for the crystal and (5.09−6.47) K for the glass.

Smoothed values of the molar heat capacity and the derived thermodynamic functions for [C_4mim][PF_6] in the condensed state are presented in Table 4 in the range (5−550 K). The derived thermodynamic functions of the liquid at 298.15 K were

$$C_{p,m} = (408.7 \pm 1.6)\ J\cdot K^{-1}\cdot mol^{-1}$$

$$\Delta_0^T S^\circ_m = (493.1 \pm 2.2)\ J\cdot K^{-1}\cdot mol^{-1}$$

$$\Delta_0^T H^\circ_m = (269.4 \pm 1.2)\ J\cdot K^{-1}\cdot mol^{-1}$$

$$\Phi^\circ_m = (223.7 \pm 2.5)\ J\cdot K^{-1}\cdot mol^{-1}.$$

The temperature corresponding to the mean value of the heat capacity in the glass transition interval from (180 to 197) K (Figure 1) was taken to be the glass transition temperature $T_g = (190.6 \pm 0.1)$ K. Its estimated uncertainty is that of a single experimental measurement without considering possible effects of sample aging. The heat capacity jump at the glass transition

$$\Delta^1_{gl} C_p \cong \Delta^1_{gl} C_s = (81.6 \pm 1.8)\ J\cdot K^{-1}\cdot mol^{-1}$$

was determined from the difference between the heat capacities of the supercooled liquid and glass, when both are extrapolated to T_g. The residual (zero-point) entropy

$$S^\circ_m(gl, T\to 0) = (14.6 \pm 3.0)\ J\cdot K^{-1}\cdot mol^{-1}$$

and enthalpy

$$H^\circ_m(gl, T\to 0) = (10.64 \pm 0.44)\ kJ\cdot mol^{-1}$$

of the glassy [C_4mim][PF_6] were determined from

$$S^\circ_m(gl, T\to 0) = -\int_{T=0}^{T_{fus}} \frac{C_p(gl,liq) - C_p(cr)}{T'}\,dT' + \frac{\Delta_{fus}\ H^\circ_m}{T_{fus}} \quad (4)$$

$$H^\circ_m(gl, T\to 0) = -\int_{T=0}^{T_{fus}} (C_p(gl,liq) - C_p(cr))\,dT' + \Delta_{fus}\ H^\circ_m \quad (5)$$

where $C_p(gl,liq)$ is the heat capacity of glass and supercooled liquid and $C_p(cr)$ is the heat capacity of the crystal.

Table 4. Molar Thermodynamic Functions of 1-Butyl-3-methylimidazolium Hexafluorophosphate (R = 8.314 472 J·K^{-1}·mol^{-1})

T/K	$C_{p,m}/R$	$\Delta_0^T H_m^\circ/RT$	$\Delta_0^T H_m^\circ/R$	Φ_m°/R	T/K	$C_{p,m}/R$	$\Delta_0^T H_m^\circ/RT$	$\Delta_0^T H_m^\circ/R$	Φ_m°/R
				Crystal					
5	0.1211	0.02959	0.03909	0.009622	130	21.99	12.63	24.45	11.82
10	0.9005	0.2321	0.3101	0.07794	140	23.23	13.34	26.13	12.78
15	2.335	0.6833	0.9333	0.2500	150	24.50	14.05	27.77	13.73
20	4.010	1.303	1.832	0.5285	160	25.81	14.74	29.39	14.65
25	5.671	2.013	2.907	0.8946	170	27.15	15.43	31.00	15.57
30	7.168	2.750	4.076	1.327	180	28.53	16.12	32.59	16.47
35	8.499	3.478	5.283	1.805	190	29.92	16.81	34.17	17.36
40	9.679	4.181	6.497	2.316	200	31.36	17.50	35.74	18.24
45	10.73	4.851	7.698	2.847	210	32.74	18.19	37.31	19.11
50	11.66	5.486	8.877	3.392	220	34.08	18.89	38.86	19.97
60	13.25	6.651	11.15	4.497	230	35.39	19.58	40.40	20.83
70	14.67	7.697	13.30	5.602	240	36.71	20.26	41.94	21.68
80	15.96	8.650	15.34	6.693	250	38.09	20.95	43.46	22.52
90	17.19	9.531	17.29	7.763	260	39.47	21.63	44.98	23.35
100	18.43	10.36	19.17	8.811	270	(40.85)[a]	22.32	46.50	24.18
110	19.62	11.15	20.98	9.835	280	(42.22)[a]	23.01	48.01	25.01
120	20.79	11.90	22.74	10.84	283.51	(42.71)[a]	23.25	48.54	25.29
				Liquid					
283.51	48.09	31.56	56.85	25.29	400	56.15	37.60	74.77	37.17
290	48.56	31.94	57.95	26.01	420	57.25	38.51	77.54	39.03
298.15	49.15	32.40	59.30	26.90	440	58.25	39.38	80.23	40.84
300	49.29	32.50	59.61	27.10	460	59.15	40.22	82.84	42.61
310	50.02	33.06	61.23	28.18	480	59.96	41.03	85.37	44.34
320	50.79	33.60	62.84	29.24	500	60.67	41.80	87.83	46.03
340	52.28	34.65	65.96	31.31	520	61.28	42.54	90.23	47.69
360	53.67	35.67	68.99	33.32	540	61.79	43.24	92.55	49.31
380	54.96	36.65	71.92	35.27	550	62.01	43.58	93.68	50.10
				Glass					
5	0.2341	0.05953	0.07902	0.01948	90	18.53	10.14	18.77	8.628
10	1.314	0.3838	0.5272	0.1435	100	19.97	11.05	20.80	9.745
15	2.880	0.9492	1.349	0.3999	110	21.40	11.93	22.77	10.84
20	4.535	1.638	2.404	0.7655	120	22.74	12.77	24.69	11.91
25	6.161	2.383	3.594	1.211	130	24.06	13.59	26.56	12.97
30	7.626	3.137	4.849	1.712	140	25.38	14.39	28.39	14.01
35	8.938	3.874	6.125	2.251	150	26.72	15.16	30.19	15.02
40	10.09	4.581	7.395	2.815	160	28.09	15.93	31.96	16.03
45	11.12	5.250	8.644	3.393	170	29.55	16.69	33.70	17.02
50	12.10	5.886	9.866	3.980	180	31.04	17.44	35.43	17.99
60	13.90	7.074	12.23	5.159	190	32.53	18.20	37.15	18.95
70	15.54	8.167	14.50	6.333	190.6	32.62	18.24	37.26	19.01
80	17.06	9.185	16.68	7.491					
				Supercooled liquid					
190.6	42.44	18.24	37.26	19.01	250	45.84	24.38	49.19	24.81
200	42.93	19.39	39.31	19.92	260	46.49	25.22	51.00	25.78
210	43.47	20.53	41.42	20.89	270	47.16	26.02	52.77	26.75
220	(44.03)[b]	21.58	43.45	21.87	280	47.85	26.79	54.50	27.71
230	(44.61)[b]	22.57	45.42	22.85	283.51	48.09	27.05	55.09	28.05
240	45.22	23.50	47.33	23.83					

[a] Extrapolated values. [b] Interpolated values.

Table 5. Density of Liquid 1-Butyl-3-methylimidazolium Hexafluorophosphate

T/K	ρ/g·cm^{-3}	T/K	ρ/g·cm^{-3}
298.23	1.36595	322.33	1.34602
302.89	1.36205	327.16	1.34202
307.90	1.35794	344.23	1.32803
312.67	1.35399	348.93	1.32435
317.58	1.34992	353.47	1.32069

The experimental values of the density of liquid [C_4mim][PF_6] (Table 5) were fitted by a simple polynomial

$$d/(\text{g·cm}^{-3}) = 1.36603 - 8.346 \times 10^{-4}(T/\text{K} - 298.15) + 2.61 \times 10^{-7}(T/\text{K} - 298.15)^2 \quad (6)$$

The densities of liquid [C_4mim][PF_6] are compared, in Figure 2, with previously reported densities.[17−19] Though our results differ systematically from published measurements by amounts that exceed our uncertainty, the present data fall in the midrange between the published data shown in Figure 2. Broadly speaking, they are 0.6% less than those by Suarez et al.[19] and 0.4% larger than those by Gu and Brennecke.[17] The densities reported by Dzyuba and Bartsch[18] do not follow the same trend as the other three data sets and deviate from this work by an amount from (−0.1 to 0.3)%. The observed differences could be attributed to varying levels of impurities, primarily H_2O and Cl^-, that were present in the samples used in this work and the published studies. Unfortunately, finding a trend has been hindered because not all authors report an analysis of impurities in their samples. However, Gu and Brennecke did report impurities of 3 ppm (mass) Cl^- and 0.0015 mass fraction H_2O (∼0.023 mol fraction) in their sample. While this report of impurities is consistent with the observation that their densities are about 0.4% lower than this work, a systematic study at different concentrations would be helpful to establish this as fact.

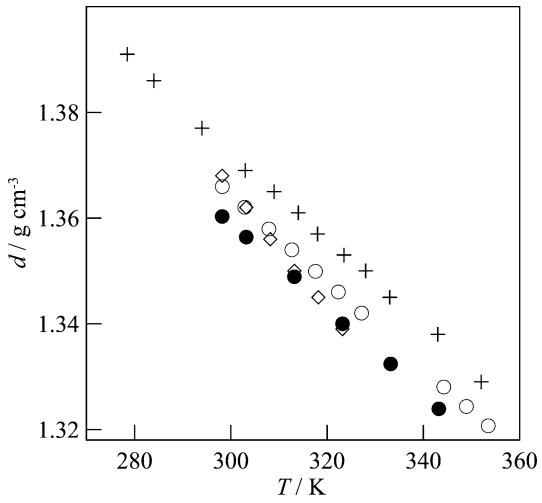

Figure 2. Temperature dependence of density of [C_4mim][PF_6]: +, Suarez et al.;[19] ●, Gu and Brennecke;[17] ◇, Dzyuba et al.;[18] ○, this work.

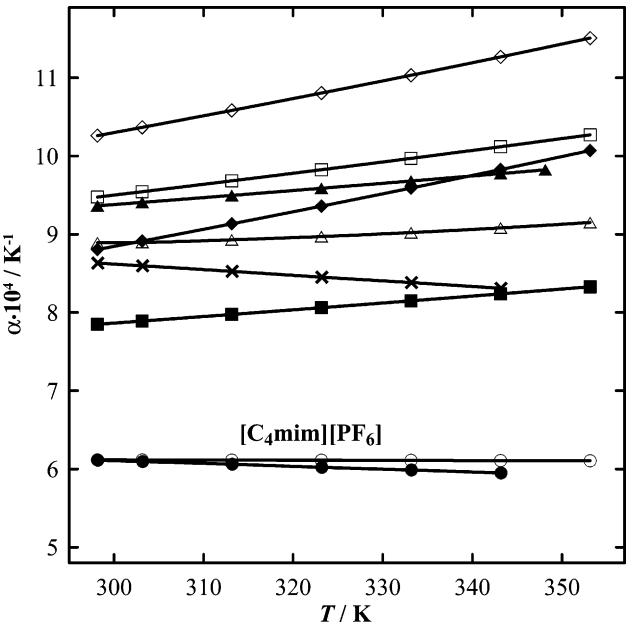

Figure 3. Temperature dependence of the thermal expansion coefficient for low molecular mass organic liquids and [C_4mim][PF_6]: ○, [C_4mim][PF_6], this work; ●, [C_4mim][PF_6];[17] △, octadecane;[20] □, butylbenzene;[20] ▲, cyclohexyl butyrate;[21] ×, 1-methyl imidazole;[17] ■, diethyl phthalate;[22] ◆, bromobenzene;[23,24] ◇, tetrachloroethene.[25]

Discussion

In the following discussion, we compare the thermodynamic properties of [C_4mim][PF_6] with those of molecular liquids of similar molecular mass and also with ionic crystals.

Density of Liquid [C_4mim][PF_6]. The reported density of liquid [C_4mim][PF_6] is much higher than that of ordinary organic liquids that do not hydrogen bond or contain heavy atoms (Cl, Br, I, etc.) in the molecules. The behavior of the thermal expansion coefficient

$$\alpha_p = \frac{1}{V}\left(\frac{\partial V}{\partial T}\right)_p$$

for liquid [C_4mim][PF_6] differs significantly from that of ordinary organic liquids, as shown in Figure 3. Values of α_p for [C_4mim][PF_6] decrease slightly (approximately 1%) with temperature in the range from (298 to 353) K. Other liquids in the comparison, except 1-methyl imidazole, show values of α_p that increase with temperature by approximately 10% over the investigated temperature range.

Thermodynamic Parameters of Fusion and the Glass Transition of [C_4mim][PF_6]. Table 6 presents a comparison of key thermodynamic parameters of both the fusion and the glass transition for a series of organic liquid substances with comparable molecular mass and [C_4mim][PF_6]. From these comparisons, we may conclude that:

1. The ratio of the temperature of fusion to the temperature of the glass transition T_{fus}/T_g, entropy of fusion $\Delta_{fus}S°$, and residual entropy $S°_m$ ($T\rightarrow 0$) [C_4mim][PF_6] are comparable to those for the organic substances.

2. The ratio $S°(T\rightarrow 0)/\Delta_{fus}S°$ for [C_4mim][PF_6] (0.21) is anomalously low. It is 30% smaller than an average value for the molecular substances (0.30) compared in Table 6. This fact suggests that glassy [C_4mim][PF_6] is more ordered than the molecular glasses in the comparison.

3. The jump in absolute heat capacity at the glass transition $\Delta^1_{gl} C_p(T_g)$ has a normal value when compared with the organic liquids. However, the relative jump in heat capacity given by

$$\frac{\Delta^1_{gl} C_p(T_g)}{C_p(\mathrm{gl}, T_g)}$$

has a value of 0.30 for [C_4mim][PF_6], which is significantly lower (between 38% and 66%) than the analogous values (ranging from 0.48 to 0.88) for the molecular substances.

At temperatures where the glassy state exists, the D parameter[34] that characterizes the fragility of liquid can be calculated with

$$D = \{(T_g/T_0) - 1\}/0.0255 = 14.8$$

where $T_0 = 138.5$ K is the Kauzmann temperature, at which the configurational entropy of liquid is equal to zero. The value of T_0 was obtained from an analysis of the temperature dependence of the configurational entropy S_{config} of liquid [C_4mim][PF_6], which was calculated with the relationship

$$S_{config}(T) = \Delta_{fus}S + \int_{T_{fus}}^{T} \frac{\{C_p(1) - C_p(\mathrm{cr})\}}{T'}\,\mathrm{d}T'$$

where C_p(l) is the heat capacity of the liquid and C_p(cr) is that of the crystal. The heat capacity of the liquid below T_g was extrapolated based on the experimental heat capacities of liquid [C_4mim][PF_6] in the temperature range from (197 to 310) K. It was noted that [C_4mim][PF_6] falls somewhere in the middle of Angell's classification scheme.[34]

Heat Capacities of Crystalline and Liquid [C_4mim][PF_6]. We compared specific heat capacities of crystalline and liquid [C_4mim][PF_6] with those of some molecular crystals and liquids. The results are shown in Figure 4. The specific heat capacity and its temperature dependence for [C_4mim][PF_6] differ significantly from those for the molecular liquids. In the temperature range from (50 to 380) K, the specific heat capacity of all the molecular liquids considered is larger than that of [C_4mim][PF_6], although the $C_p = f(T)$ curves for these substances have quite different shapes.

The feature that distinguishes crystalline [C_4mim][PF_6] is that its specific heat capacity below 50 K decreases at a rate considerably slower than that for the specific heat capacities of the molecular crystals (Figure 4). A possible

Table 6. Thermodynamic Parameters of Fusion and Glass Transition for Some Molecular Organic Compounds and [C_4Mim][PF_6]

compound [ref]	T_{fus} / K	$\Delta_{fus}S$ / J·K^{-1}·mol^{-1}	T_g / K	T_g/T_{fus}	$\Delta^1_{gl}C_P(T_g)$ / J·K^{-1}·mol^{-1}	$\Delta^1_{gl}C_P(T_g)/C_P$(gl, T_g)	$S°(T\rightarrow 0)$ / J·K^{-1}·mol^{-1}	$S°(T\rightarrow 0)$ / J·K^{-1}·mol^{-1}
2-methylpentane [26]	119.6	52.4	78.9	0.66	67.4	0.88	17.7	0.34
3-bromopentane [27]	167.3	50.2	107.4	0.64	76.4	0.78	16.4	0.33
cyclohexyl formate [28]	201.3	52.1	140.0	0.70	87.9	0.84	13.2	0.25
cyclohexyl acetate [28]	224.6	59.2	151.8	0.68	87.1	0.69	16.0	0.27
methyl *m*-toluate [29]	270.6	63.3	166.5	0.62	78.2	0.57	22.4	0.35
isopropylbenzene [30]	177.1	41.4	126.0	0.71	75.2	0.73	12.0	0.29
cyclohexyl butyrate [28]	219.6	75.5	145.2	0.66	115.2	0.66	22.1	0.29
cyclohexyl valerate [28]	222.4	82.4	145.8	0.66	126.1	0.67	24.9	0.30
dimethyl phthalate [10]	274.2	61.8	190.3	0.69	92.2	0.50	16.8	0.27
diethyl phthalate [31]	269.9	66.7	180.8	0.67	115.0	0.53	23.0	0.34
benzophenone [32]	321.0	56.7	218.0	0.68	86.1	0.52		
o-terphenyl [33]	329.3	52.2	242.4	0.74	109.2	0.48		
mean value				0.68				0.30
[C_4mim][PF_6]	283.5	69.1	190.6	0.67	81.6	0.30	14.6	0.21

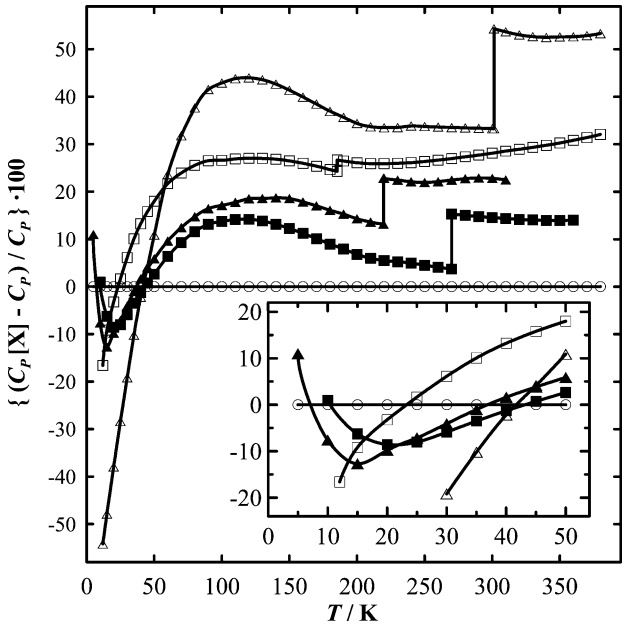

Figure 4. Relative deviation (%) of specific heat capacities of crystals and liquids of some molecular organic substances (C_p[X]) from specific heat capacities of crystalline and liquid [C_4mim][PF_6] (C_p). ○, [C_4mim][PF_6], this work; △, octadecane;[35] □, butyl benzene;[36] ▲, cyclohexyl butyrate;[28] ■, diethylphthalate;[31] vertical lines designate the temperatures of fusion of corresponding substances.

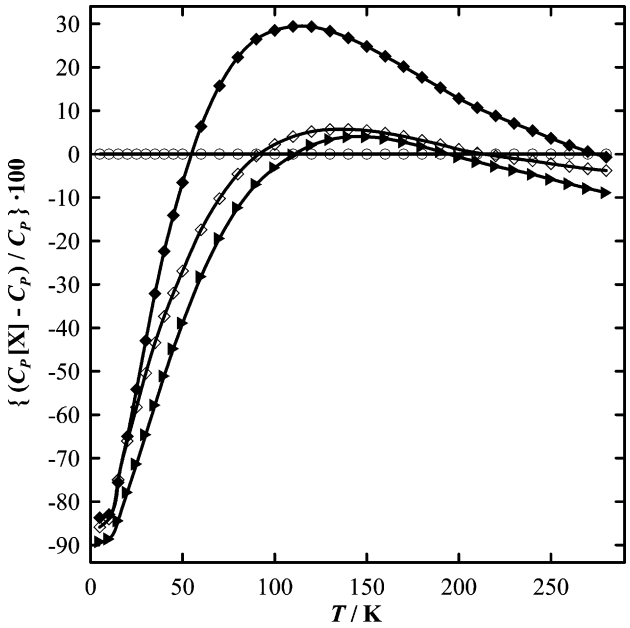

Figure 5. Relative deviation (%) of specific heat capacities of the crystals of hydroxylammonium salts (C_p[X])[37] from specific heat capacity of crystalline [C_4mim][PF_6]: ○, [C_4mim][PF_6], this work; ◆, (NH_2OH)·HCl; ◇, $(NH_2OH)_2$·H_2SO_4; ▲, $(NH_2OH)_3$·H_3PO_4.

explanation for this anomaly is related to the relatively low characteristic Debye temperature ($\theta_D = 62.7$ K) for [C_4mim][PF_6]. The quantity θ_D depends on mechanical properties of the crystal and provides some evidence of relatively low packing density of ions in its lattice. Though crystalline cyclohexyl butyrate[28] has a close, but slightly higher, Debye temperature ($\theta_D = 71.3$ K), the temperature dependence of its specific heat capacity differs significantly from that for [C_4mim][PF_6].

A second possible explanation of this anomaly is that, at temperatures below 40 K, the electronic contribution to the specific heat capacity may be unusually large when compared with the lattice contribution.

In a second comparison, shown in Figure 5, we compare the specific heat capacities of crystalline [C_4mim][PF_6] with those of ionic crystals, specifically hydroxylammonium salts.[37] It is clear that, at temperatures below 50 K, the rate of decrease of the specific heat capacity of [C_4mim][PF_6] is considerably smaller than that of the ionic crystals. This could be explained by an unusually large electronic contribution to the heat capacity of [C_4mim][PF_6] at temperatures below 40 K. Published work on the ionic crystal pyridinium hexafluorophosphate[38] ([PyH][PF_6]), which is similar in structure to [C_4mim][PF_6], shows that its specific heat capacity ($T < 40$ K) decreases at an even slower rate (Figure 6).

The anomalous thermal behavior of [C_4mim][PF_6] below 50 K would lead to relatively large errors in an extrapolation of C_p from temperatures near 100 K to 0 K. Such extrapolations are often done by using a comparative method, in this case by using molecular compounds for comparison. Before the measurements ($T < 100$ K) reported here were completed, we extrapolated[5] the heat capacity of the [C_4mim][PF_6] crystal by using published data for pentadecanolactone[10] (PDL) as a guide, to give an estimate for the entropy at 100 K of

$$(S°_{100}(\mathrm{cr}) - S°_0(\mathrm{cr}))_{\mathrm{estim}} = 139\ \mathrm{J{\cdot}K^{-1}{\cdot}mol^{-1}}$$

a value that is 13% lower than our present recommendation

$$(S°_{100}(\mathrm{cr}) - S°_0(\mathrm{cr}))_{\mathrm{exp}} = 159.4\ \mathrm{J{\cdot}K^{-1}{\cdot}mol^{-1}}$$

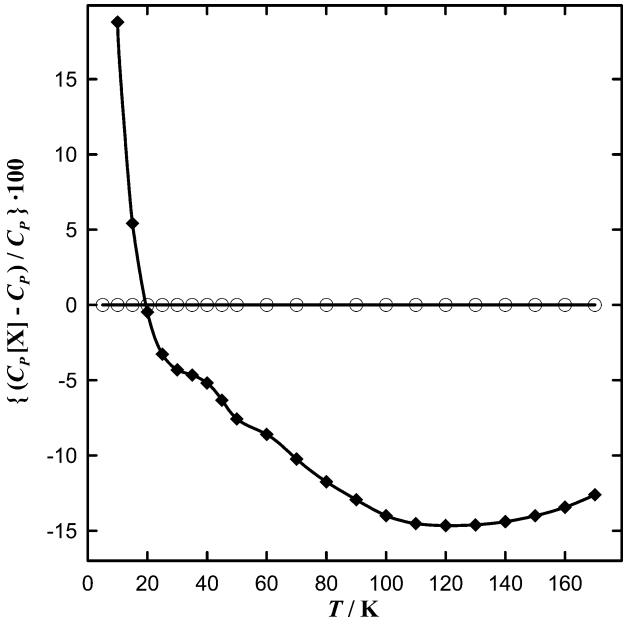

Figure 6. Relative deviations (%) of specific heat capacity of the crystal of pyridinium hexafluorophosphate[38] (C_p[X]) from specific heat capacity of crystalline [C_4mim][PF_6]. ○, [C_4mim][PF_6]; ◆, [PyH][PF_6].

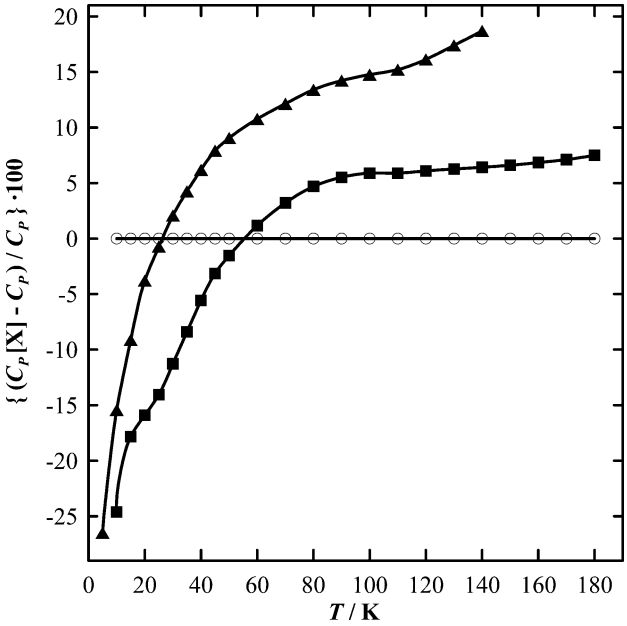

Figure 7. Relative deviation (%) of specific heat capacities of low molecular mass glasses (C_p[X]) from C_p of glassy [C_4mim][PF_6]: ○, [C_4mim][PF_6], this work; ▲, cyclohexyl butyrate;[28] ■, diethyl phthalate.[31]

In the earlier work, we used estimated entropies at 25 °C and applied a thermodynamic relationship for ideal gases to estimate a value for the vapor pressure at this temperature. When we use the new value for $\Delta_{vap}S°$(298.15 K) = 175.3 J·K^{-1}·mol^{-1}, and a new value $\Delta_{vap}H°$(298.15 K) = 145 kJ·mol^{-1} reported by Morrow and Maginn,[39] obtained by a molecular dynamics simulation, we obtain $P_{sat} \approx 10^{-11}$ Pa at a temperature of 298.15 K.

Heat Capacity of Glassy [C₄mim][PF₆]. The specific heat capacities of glassy [C_4mim][PF_6], diethyl phthalate[31] and cyclohexyl butyrate[28] are compared in Figure 7. It was no surprise that the observed trend is the same as that of the crystalline substances. The specific heat capacity of glassy [C_4mim][PF_6] decreases at a rate considerably slower

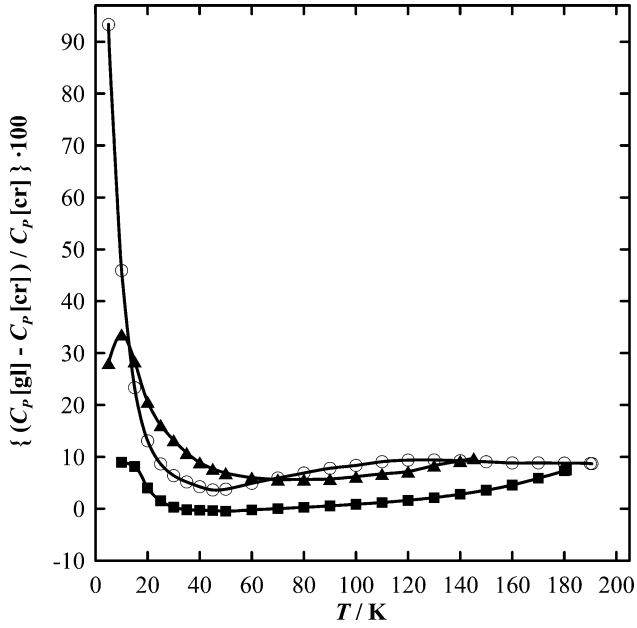

Figure 8. Relative difference of the heat capacities of glass C_p-[gl] and crystal C_p[cr]: ○, [C_4mim][PF_6], this work; ▲, cyclohexyl butyrate,[28] ■, diethyl phthalate.[31] Data below T_g are shown.

than that of the molecular substances at temperatures below 50 K. In Figure 8, we compare the differences of heat capacities of glass and the crystal, given by

$$\frac{C_p(\text{gl}) - C_p(\text{cr})}{C_p(\text{cr})} 100\ (\%)$$

which shows a similar behavior at temperatures as low as 20 K, but a divergence below this temperature. At temperatures T < 20 K, the specific heat capacity for glassy [C_4mim][PF_6] decreases with temperature at a rate much slower than that of its crystalline form.

In summary, the salient features of thermodynamic properties of [C_4mim][PF_6] are

1. Compared to molecular substances, smaller specific heat capacity of crystal, glass, and liquid at temperatures above 50 K.

2. Anomalously slow decrease with temperature of the specific heat capacity of crystalline and glassy [C_4mim][PF_6] in a range below 50 K.

Acknowledgment

The authors wish to thank Jason Widegren for a thorough and detailed purity analysis of the [C_4mim][PF_6] sample.

Supporting Information Available:

The entire set of heat capacity measurements made with the scanning heat bridge calorimeter at approximately 1500 conditions. This material is available via the Internet at http://pubs.acs.org.

Literature Cited

(1) Welton, T. Room-Temperature Ionic Liquids. Solvents for Synthesis and Catalysis. *Chem. Rev.* **2000**, *99*, 2071−2083.
(2) Fadeev, A. G.; Meagher, M. M. Opportunities for Ionic Liquids in Recovery of Biofuels. *Chem. Commun.* **2001**, 295.
(3) Blanchard, L. A.; Gu, Z.; Brennecke, J. F. High-Pressure Phase Behavior of Ionic Liquid/CO_2 Systems. *J. Phys. Chem. B* **2001**, *105*, 2437.
(4) Brennecke, J. F.; Maginn, E. J. Ionic Liquids: Innovative Fluids for Chemical Processing. *AIChE J.* **2001**, *47*, 2384−2389.

(5) Paulechka, Y. U.; Kabo, G. J.; Blokhin, A. V.; Vydrov, O. A.; Magee, J. W.; Frenkel, M. Thermodynamic Properties of 1-Butyl-3-methylimidazolium Hexafluorophosphate in the Ideal Gas State. *J. Chem. Eng. Data.* **2003**, *48*, 457−462.
(6) Kosov, V. I.; Malyshev, V. M.; Milner, G. A.; Sorkin, E. L.; Shibakin, V. F. Multi-Purpose Setup for Thermophysical Measurements Controlled with a Microcomputer. *Izmer. Tekh.* **1985**, *11*, 56−58.
(7) Kabo, G. J.; Kozyro, A. A.; Marchand, A.; Diky, V. V.; Simirsky, V. V.; Ivashkevich, L. S.; Krasulin, A. P.; Sevruk, V. M.; Frenkel, M. L. Thermodynamic Properties of Heptacyclotetradecane $C_{14}H_{16}$. *J. Chem. Thermodyn.* **1994**, *26*, 129−142.
(8) Pavese, F.; Malyshev, V. M. Routine Measurements of Specific Heat Capacity and Thermal Conductivity of High-T_c Superconducting Materials in the Range 4−300 K Using Modular Equipment. *Adv. Cryog. Eng.* **1994**, *40*, 119−124.
(9) Furukawa, G. T.; McCoskey, R. E.; King, G. J. Calorimetric Properties of Benzoic Acid from 0 to 410 K. *J. Res. Natl. Bur. Stand.* **1951**, *47*, 256−261.
(10) Vasiliev, I. A.; Petrov, V. M. *Thermodynamic Properties of Oxygen-Containing Organic Compounds*; Khimiya: Leningrad, 1984; p 240.
(11) White, G. K.; Collocott, S. J. Heat Capacity of Reference Materials: Cu and W. *J. Phys. Chem. Ref. Data* **1984**, *13*, 1251−1257.
(12) Kabo, G. J.; Diky, V. V.; Kozyro, A. A.; Krasulin, A. P.; Sevruk, V. M. Thermodynamic Properties, Conformational Composition, and Phase Transitions of Cyclopentanol. *J. Chem. Thermodyn.* **1995**, *27*, 953−967.
(13) Diky, V. V.; Kabo, G. J.; Kozyro, A. A.; Krasulin, A. P.; Sevruk, V. M. Thermodynamic Properties of Crystalline and Liquid Chlorocyclohexane and Inversion of Ring. *J. Chem. Thermodyn.* **1994**, *26*, 1001−1013.
(14) Parks, G. S.; Kennedy, W. D.; Gates, R. R.; Mosley, J. R.; Moore, G. E., Renquist, G. E. Thermal Data on Organic Compounds. XXVI. Some Heat Capacity, Entropy, and Free Energy Data for Seven Compounds Containing Oxygen. *J. Am. Chem. Soc.* **1956**, *78*, 56−59.
(15) Kobashi, K.; Oguni, M. Heat Capacities of Chlorocyclohexane and Bromocyclohexane between the Temperatures 10 K and 300 K, and Phase Transitions in the Crystalline State for Chlorocyclohexane. *J. Chem. Thermodyn.* **1995**, *27*, 979−990.
(16) Kabo, A. G.; Diky, V. V. Detailes of Calibration of a Scanning Calorimeter of the Triple-Heat Bridge Type. *Thermochim. Acta* **2000**, *347*, 79−84.
(17) Gu, Zh.; Brennecke, J. F. Volume Expansivities and Isothermal Compressibilities of Imidazolium and Pyridinium-Based Ionic Liquids. *J. Chem. Eng. Data.* **2002**, *47*, 339−345.
(18) Dzyuba, S. V.; Bartsch, R. A. Influence of Structural Variations in 1-Alkyl(aralkyl)-3-methylimidazolium Hexafluorophosphates and Bis(trifluoromethylsulfonyl)imides on Physical Properties of the Ionic Liquids. *Chem. Phys. Chem.* **2002**, *3*, 161−166.
(19) Suarez, P. A. Z.; Einloft, S.; Dullius, J. E. L.; de Souza, R. F.; Dupont, J. Synthesis and Physical-Chemical Properties of Ionic Liquids Based on 1-*n*-Butyl-3-methylimidazolium Cation. *J. Chim. Phys.* **1998**, *95*, 1626−1639.
(20) *Hydrocarbons* (*d*-tables). TRC Thermodynamic Tables.
(21) Kabo, G. J.; Blokhin, A. V.; Paulechka, Y. U. Thermodynamic Properties of Cyclohexyl Esters and the Influence of the Process of Hole Formation in Liquids to their Thermodynamic Parameters of Phase Transitions and the Glass Transition. *Selected works of the Belarusian State University. Vol. V, Chemistry*; BSU: Minsk, 2001; pp 382−400.
(22) Perkin, W. H. LXIX. On Magnetic Rotatory Power, Especially of Aromatic Compounds. *J. Chem. Soc.* **1896**, *69*, 1025−1035.
(23) Nayar, S.; Kudchadker, A. P. Densities of Some Organic Substances. *J. Chem. Eng. Data* **1973**, *18*, 356−360.
(24) Korosi, G.; Kovats, E. Density and Surface Tension of 83 Organic Liquids. *J. Chem. Eng. Data*, **1981**, *26*, 323−347.
(25) Afenkov, N. I. Measurement of Specific Volume of Some Organic Liquids by an Adjustable Dilatometer. *Izv. Vyssh. Uchebn. Zaved., Khim. Khim. Tekhnol.* **1958**, 128−132.
(26) Douslin, D. R.; Huffman, H. M. Low-Temperature Thermal Data of the Five Isomeric Hexanes. *J. Am. Chem. Soc.* **1946**, *68*, 1704−1708.
(27) Takahara, S.; Yamamuro, O.; Matsuo, T. Calorimetric Study of 3-Bromopentane: Correlation between Structural Relaxation Time and Configurational Entropy. *J. Phys. Chem.* **1995**, *99*, 9589−9592.
(28) Kozyro, A. A.; Blokhin, A. V.; Kabo, G. J.; Paulechka, Y. U. Thermodynamic Properties of Some Cyclohexyl Esters in the Condensed State. *J. Chem. Thermodyn.* **2001**, *33*, 305−331.
(29) Blokhin, A. V.; Paulechka, Y. U.; Kabo, G. J.; Kozyro A. A. Thermodynamic Properties of Methyl Esters of Benzoic and Toluic Acids in the Condensed State. *J. Chem. Thermodyn.* **2002**, *34*, 29−55.
(30) Kishimoto, K.; Suga, H.; Seki, S. Calorimetric Study of the Glassy State. VIII. Heat Capacity and Relaxational Phenomena of Isopropylbenzene. *Bull. Chem. Soc. Jpn.* **1973**, *46*, 3020−3031.
(31) Chang, S. S.; Horman J. A.; Bestul, A. B. Heat Capacities and Related Thermal Data for Diethyl Phthalate Crystal, Glass and Liquid to 360 K. *J. Res. Natl. Bur. Stand. Phys. Chem.* **1967**, *71A*, 293−305.
(32) De Kruif, C. G.; van Miltenburg, J. C.; Blok, J. G. Molar Heat Capacities and Vapour Pressure of Solid and Liquid Benzophenone. *J. Chem. Thermodyn.* **1983**, *15*, 129−136.
(33) Chang, S. S.; Bestul, A. B. Heat Capacity and Thermodynamic Properties of *o*-Terphenyl Crystal, Glass, and Liquid. *J. Chem. Phys.* **1972**, *56*, 503−516.
(34) Angell, C. A. Relaxation in Liquids, Polymers and Plastic Crystals−Strong/Fragile Patterns and Problems. *J. Non-Cryst. Solids* **1991**, *131−133*, 13−31.
(35) Messerly, J. F.; Guthrie, G. B.; Todd, S. S.; Finke, H. L. Low-Temperature Thermal Data for *n*-Pentane, *n*-Heptadecane, and *n*-Octadecane. Revised Thermodynamic Functions for the *n*-Alkanes, C_5−C_{18}. *J. Chem. Eng. Data* **1967**, *12*, 338−346.
(36) Messerly, J. F.; Todd, S. S.; Finke, H. L. Low-Temperatures Thermodynamic Properties of *n*-Propyl and *n*-Butylbenzenes. *J. Phys. Chem.* **1965**, *69*, 4304−4311.
(37) Krouk, V. S.; Kabo, G. J.; Blokhin, A. V.; Diky, V. V.; Paulechka, Y. U. The Heat Capacity of Hydroxylammonium Chloride, Sulphate, and Phosphate. *Thermochim. Acta* **2002**, *389*, 11−18.
(38) Hanaya, M.; Ohta, N.; Oguni, M. Calorimetric Study of Phase Transitions in Pyridinium Iodide and Pyridinium Hexafluorophosphate Crystals. *J. Phys. Chem. Solids* **1993**, *54*, 263−269.
(39) Morrow, T. I.; Maginn, E. J. Molecular Dynamics Study of the Ionic Liquid 1-*n*-Butyl-3-methylimidazolium Hexafluorophosphate. *J. Phys. Chem.* **2002**, *49*, 12807−12813.

Received for review May 31, 2003. Accepted February 25, 2004. The authors are grateful to the Belarusian Republican Foundation for Fundamental Research for financial support of this work (Grant Kh03MS-029).

JE034102R